Chemical Science

ROYAL SOCIETY OF CHEMISTRY

EDGE ARTICLE

View Article Online
View Journal | View Issue

Cite this: *Chem. Sci.*, 2021, **12**, 3674

All publication charges for this article have been paid for by the Royal Society of Chemistry

Discovery of rare sulfated *N*-unsubstituted glucosamine based heparan sulfate analogs selectively activating chemokines†

Prashant Jain,‡[b] Chethan D. Shanthamurthy,‡[b] Shani Leviatan Ben-Arye,[a] Robert J. Woods,[c] Raghavendra Kikkeri*[b] and Vered Padler-Karavani *[a]

Received 24th October 2020
Accepted 15th January 2021

DOI: 10.1039/d0sc05862a

rsc.li/chemical-science

Achieving selective inhibition of chemokines with structurally well-defined heparan sulfate (HS) oligosaccharides can provide important insights into cancer cell migration and metastasis. However, HS is highly heterogeneous in chemical composition, which limits its therapeutic use. Here, we report the rational design and synthesis of *N*-unsubstituted (NU) and *N*-acetylated (NA) heparan sulfate tetrasaccharides that selectively inhibit structurally homologous chemokines. HS analogs were produced by divergent synthesis, where fully protected HS tetrasaccharide precursor was subjected to selective deprotection and regioselectively *O*-sulfated, and *O*-phosphorylated to obtain 13 novel HS tetrasaccharides. HS microarray and SPR analysis with a wide range of chemokines revealed the structural significance of sulfation patterns and NU domain in chemokine activities for the first time. Particularly, **HT-3,6S-NH** revealed selective recognition by CCL2 chemokine. Further systematic interrogation of the role of **HT-3,6S-NH** in cancer demonstrated an effective blockade of CCL2 and its receptor CCR2 interactions, thereby impairing cancer cell proliferation, migration and invasion, a step towards designing novel drug molecules.

Introduction

Chemokines are endogenous signaling peptides essential for immuno-surveillance, homeostasis, inflammation, infection and tissue repair.[1] Chemokines and their receptor activities depend on how they bind and oligomerize in the presence of glycosaminoglycans (GAGs).[2] Humans express 47 chemokines and 20 receptors, and most of the chemokines are highly basic proteins. It has been therefore hypothesized elsewhere that chemokine–GAG binding is non-specific. However, after the discovery of acidic CCL3 and CCL4 chemokines binding to GAGs, it had become clearer that their interaction proceeds in a sequence-dependent manner.[3] Moreover, chemokines have shown different interaction strengths with various GAGs, including heparan sulfate (HS), chondroitin sulfate and dermatan sulfate, illustrating that microheterogeneity in GAG structures can modulate binding patterns, for example through uronic acid composition, sulfation patterns and oligosaccharide length.[4]

This has prompted the synthesis of well-described, homogeneous GAG structures, and more specifically HS oligosaccharides, to regulate chemokine activity. For example, Gallagher *et al.* reported that the CXCL4 chemokine requires HS 2-*O*-sulfated iduronic acid (IdoA) for tetramerization and binding to its cell surface receptors.[5] Elsewhere, Lindahl *et al.* had shown that interleukin-8 (CXCL8 or IL-8) prefers the IdoA(2-OSO_3^-)-GlcNSO_3^-(6OSO_3^-) repeating unit to activate neutrophil trafficking,[6] while Gardiner *et al.* reported the elegant role of 6-*O*-sulfation in switching the binding between CXCL12 and IL-8.[7] Hesieh-Wilson *et al.* demonstrated that the trisulfated IdoA(2-OSO_3^-)-GlcNSO_3^-(6-OSO_3^-)-conjugated polymer strongly inhibited RANTES (CCL5)-CCR3-receptor-mediated cell migration.[8] In addition, Seeberger *et al.* showed that CCL21 strongly binds to a hexasaccharide containing the GlcNSO_3^-(6-OSO_3^-)-IdoA(2-OSO_3^-) repeating unit as compared to CXCL12, while CCL19 does not bind to it at all.[9] Boons *et al.* discovered that CCL2 binds to highly sulfated HS compounds and exhibits no preference for the uronic acid component, while both CCL2 and CCL13 displayed promiscuous binding with most of the HS glycans.[10] These data suggest that well-defined HS oligosaccharides can provide structural details to target chemokine–GAG interaction to modulate its activities. However, HS is highly heterogeneous in its structure and the majority of the HS libraries that have been used for chemokine studies are

[a]*Department of Cell Research and Immunology, The Shmunis School of Biomedicine and Cancer Research, The George S. Wise Faculty of Life Sciences, Tel Aviv University, Tel Aviv, 69978, Israel. E-mail: vkaravani@tauex.tau.ac.il*

[b]*Department of Chemistry, Indian Institute of Science Education and Research, Pune-411008, India. E-mail: rkikkeri@iiserpune.ac.in*

[c]*Complex Carbohydrate Research Center, University of Georgia, Athens 30606, GA, USA*

† Electronic supplementary information (ESI) available. See DOI: 10.1039/d0sc05862a

‡ Equal contribution.

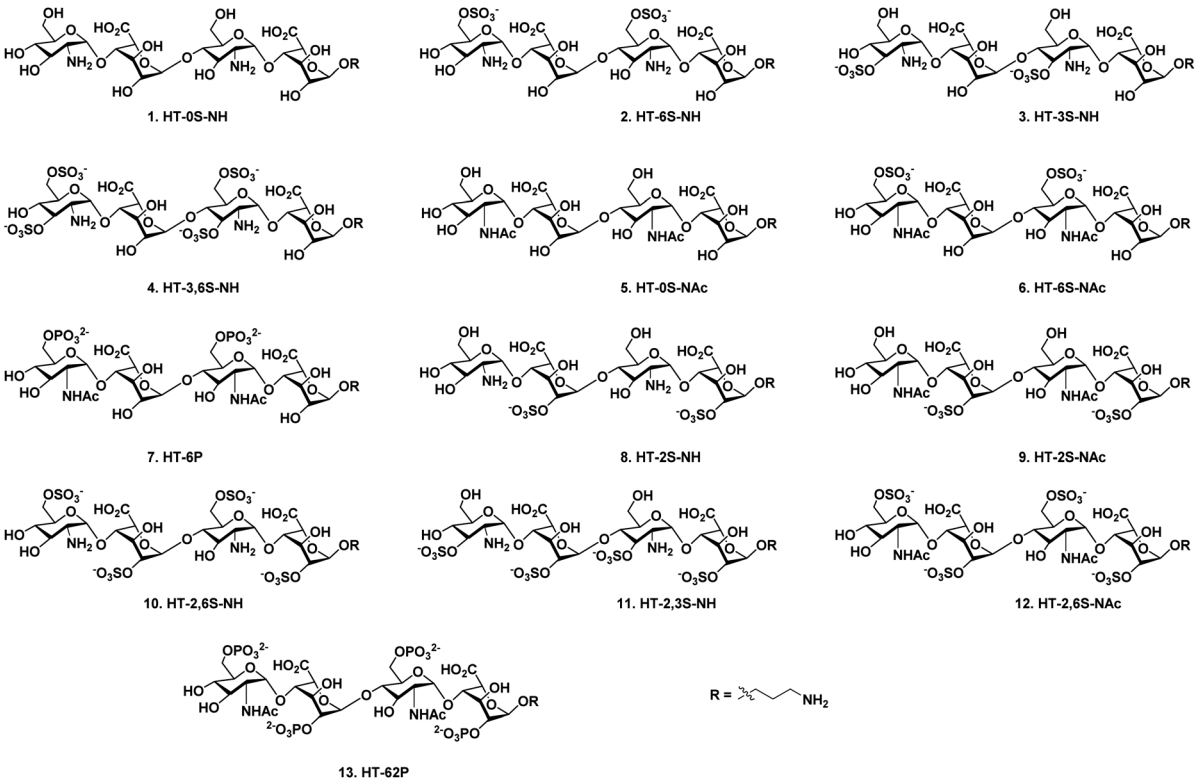

Fig. 1 Structures of heparan sulfate tetrasaccharide analogs (**1–13**).

composed of *N*-sulfated and *N*-acetylated (NA) glucosamine domains.[8–10] Native HS also expresses an *N*-unsubstituted (NU) domains, but this region has not been fully investigated in existing studies.[11] To address this gap, and to decipher the sulfation code of chemokine heparin binding, here we report the divergent synthesis of a limited number of NU- and NA domains HS tetrasaccharides (Fig. 1).

High-throughput screening of these synthetic HS ligands with a wide range of chemokines revealed selective chemokine binder, which can be used to block chemokine activity to target cancer biology. However thus far, only few heparin binding proteins have been reported to bind NU-domain-containing HS ligands,[12] and here we provide the first such example where chemokines activity was interrogated systematically with NU domain ligands.

Results and discussion

N-unsubstituted and *N*-acetylated HS analog library with regioselective sulfate modifications at 2-*O* (IdoA), 3-*O* (GlcN), and 6-*O* (GlcN) were obtained by single tetrasaccharide **27** and its *N*-acetate counterpart **28** (Scheme 1) using the divergent synthetic approach. Synthesis of **27** required a carefully designed technique that allowed us to do selective site modifications along the tetrasaccharide backbone in a controlled manner. Efforts led by various research groups revolutionized heparin sulfate synthesis in the past decade.[13] Using a similar strategy as Hung[13h] *et al.* with slight modifications in the protecting group, synthesis of **27** was carried out by disaccharide building blocks **21** and **18**. Notably, the use of 4-*O*-chloroacetate (ClA) at non reducing GlcN residue as a temporary protecting group in **17** was found to be vital for chain elongation than other previously reported 4-*O* protecting groups such as Lev[13f]/Fmoc[13m]/TCA.[13r] Disaccharides (**21** and **18**) and monosaccharide precursors were synthesized from glucosamine and iduronic acid building blocks **14**, **16**, **19** & **20**, as previously described.[13h,14] Next, we adopted [2 + 2] glycosylation approach with **21** (glycosyl donor) and **18** (glycosyl acceptor) to obtain 1,6 anhydrous tetrasaccharide **22** in excellent yield. Acetolysis of the reducing end IdoA residue of **22** with the aid of acetic anhydride and copper trifluoromethanesulfonate as catalyst followed by phenyl trimethylsulfide and ZnI_2 treatment afforded **24** as a thiophenol glycosyl donor. Linker glycosylation of **24**, followed by sequential deacetylation and TEMPO mediated oxidation of **25**, yielded **27** (72% for three steps). Finally, C-2 azide of glucosamine moieties in **27** was converted into acetate in the presence of Zn/AcOH/Ac_2O to develop tetrasaccharide **28**, which was further used to synthesize HS analogs with *N*-acetate backbone (Scheme 1).

A divergent synthetic approach was followed to develop a combinatorial library of HS oligosaccharides. For instance, silyl protecting group TBDPS was deprotected selectively using 70% HF·py for 6-*O*-sulfate derivatives precursors (**29** & **36**). Similarly, NAP deprotection with the help of DDQ yielded 3-*O*-sulfated precursors (**31** & **34**). The lactone ring was first opened for the derivatives carrying 2-*O*-sulfated IdoA, followed by the benzyl esterification to yield **39** & **42** in moderate yield (Scheme

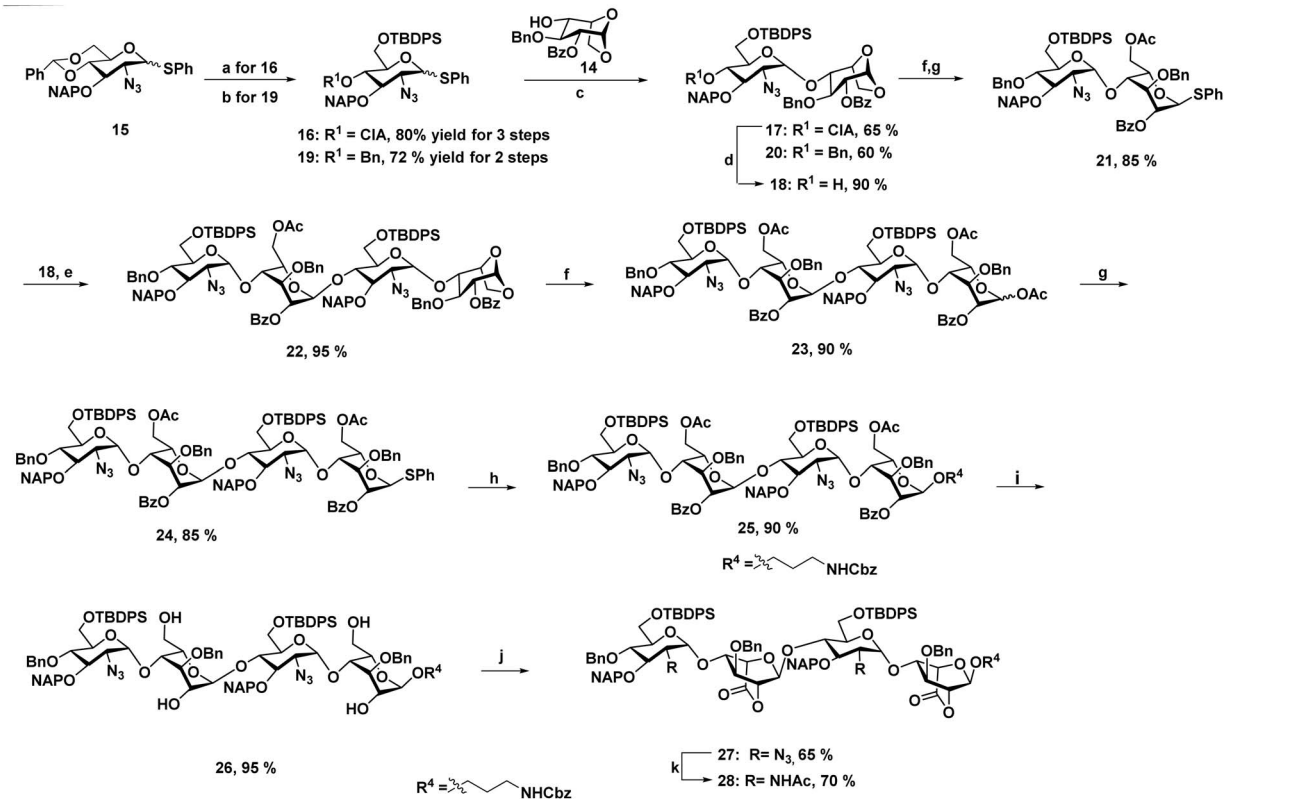

Scheme 1 (a) (i) PTSA, CH_2Cl_2/MeOH (1 : 2), rt, 6 h; (ii) TBDPSCl, imidazole, DMAP, CH_2Cl_2, 0 °C, 12 h; (iii) $(ClAc)_2O$, CH_2Cl_2/py (4 : 1), 0 °C, 20 min. (b) (i) BH_3·THF, TMSOTf, CH_2Cl_2, 0 °C, 6 h; (ii) TBDPSCl, imidazole, DMAP, CH_2Cl_2, 0 °C, 12 h. (c) NIS, TMSOTf, 4 Å MS, −78 °C to −20 °C, CH_2Cl_2, 30 min. (d) Thiourea, MeOH/py (1 : 1), 80 °C, 1 h. (e) NIS, TMSOTf, 4 Å MS -10 °C, CH_2Cl_2, 30 min. (f) Ac_2O, $Cu(OTf)_2$, rt, 12 h. (g) TMSSPh, ZnI_2, CH_2Cl_2, rt, 2 h. (h) Benzyl (3-hydroxypropyl)carbamate, NIS, TfOH, 4 Å MS, rt, CH_2Cl_2, 30 min. (i) NaOMe, CH_2Cl_2/MeOH (1 : 1), rt, 12 h. (j) TEMPO, CH_2Cl_2/MeOH (1 : 1), rt, 12 h. (k) Zn, THF/AcOH/Ac_2O (3 : 2:2), rt, 12 h.

2). Subsequent, selective deprotection was carried out in a similar manner for oligosaccharides having multiple *O*-2,6 or *O*-2,3 sulfate modifications (**45**, **47** & **50**). $SO_3 \cdot NEt_3$ was used for introducing sulfate group in the backbone (**30**, **32**, **35**, **37**, **40**, **43**, **46**, **48** & **51**), whereas for the phosphate derivative (**38** & **52**) diphenylphsphoryl chloride (DPPC) was utilized. Finally, global deprotection of all the sulfated derivatives, including non-sulfated analogs (**29** & **36**) yielded desired HS tetrasaccharide **1–13** with the amine linker at the reducing for the generation of HS microarray. Final HS oligosaccharides and intermediates were characterized by ^1H, ^{13}C, DEPT and ^{31}P NMR. Additionally, molecular weights for all the compounds were confirmed by high-resolution mass spectroscopy.

To unravel HS–chemokines binding patterns, heparin microarray was fabricated and examined with various biotinylated chemokines, at three different concentrations, followed by detection with Cy3-tagged streptavidin. We interrogated the binding of HS analogs on three homeostatic chemokines (CCL28, CXCL12 and CCL21) and six inflammatory chemokines [CXCL8 (IL-8), CXCL10 (IP-10), CCL2 (MCP-1) CCL7 (MCP-3), CCL13 (MCP-4) and CCL5 (RANTES)]. To rationalize the binding patterns of oligosaccharides, each HS–chemokines interaction was ranked according to percentage of maximal binding. Based on ranking and chemokine binding patterns, they were segregated into four groups (A, B, C and D) (Fig. 2a).

In this analysis, CCL13 (an inflammatory chemokine), CXCL12 and CCL21 (homeostatic chemokine) shared several of the conserved binding patterns, which suggest that these chemokines share several homologous binding pockets. For instance, group A chemokines bind to non-sulfated **HT-0S-NH** and phosphorylated ligands (**HT-6,2P** and **HT-6P**) (Fig. 2a), suggesting that the HS-based structure–activity relationship of these chemokines do not solely depend on the sulfate group. Moreover, group A chemokines showed strong binding with di-sulfated analogs such as **HT-2S-NH** and **HT-6S-NAc**. However, its respective NU and NA counterpart (**HT-6S-NH** and **HT-2S-NAc**) displayed weak binding (Fig. 2a), illustrating that NU and NA domains display switchable binding patterns *via* sulfation codes. It is noted that highly sulfated HS ligands displayed moderate to strong binding regardless of sulfation pattern or NU/NA domains. These trends clearly demonstrate that group A chemokines are sensitive to di-sulfation codes, while the highly sulfated HS ligands may improve the binding strength, but with poor selectivity.

In group B, CCL28 chemokine displayed weak binding with non-sulfated analogs (ranked 36% for **HT-0S-NH** and 22% **HT-0S-NAc**) and moderate to strong binding with sulfated ligands. Unlike, group A chemokines, CCL28 displayed poor binding with 2-*O*-sulfated NU ligand (ranked 43% for **HT-2S-NH**). Whereas, **HT-6S-NAc** (ranked 79%) and **HT-3S-NH** (ranked 62%)

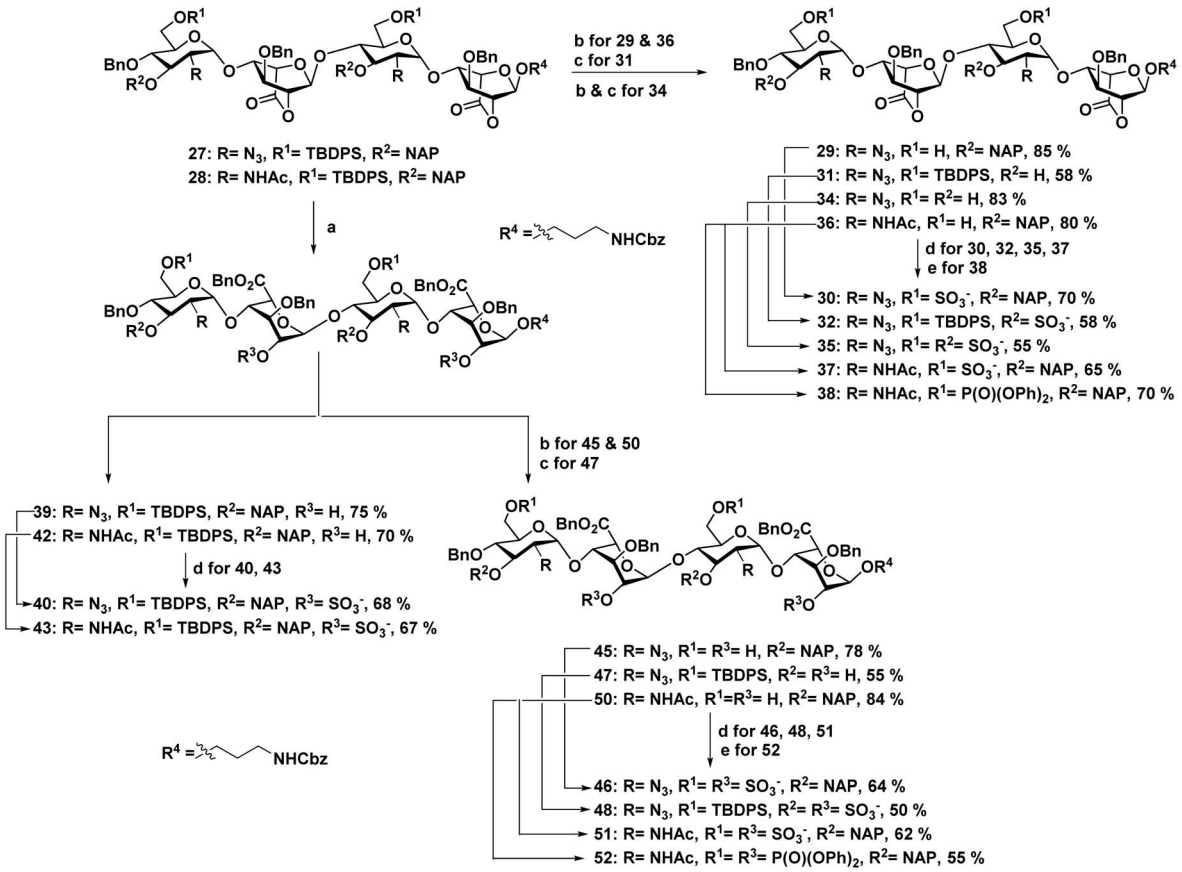

Scheme 2 (a) (i) $LiOH \cdot H_2O$, THF/H_2O (1 : 1), rt, 2 h; (ii) BnBr, TBAI, $NaHCO_3$, DMF, 60 °C, 2 h. (b) 70% HF·py, py, 0 °C, 12 h. (c) DDQ, CH_2Cl_2/H_2O (18 : 1), rt, 1 h. (d) $SO_3 \cdot NEt_3$, DMF, 60 °C, 72 h. (e) DPPC, DMAP, NEt_3, CH_2Cl_2/py (1 : 1), 0 °C, 12 h.

di-sulfated ligands, **H-2,6S-NH** (ranked 79%), **HT-2,6-NAc** (ranked 66%), **HT-3,6S-NH** (ranked 54%) tetra-sulfated ligands and **HT-2,6P** (ranked 78%) phosphate ligand displayed moderate to strong binding (Fig. 2a). These results suggest that group A and group B chemokine binding patterns may require a more complex HS library to establish selectivity.

In group C, CCL7 and CXCL10 displayed a sulfation pattern-based binding. Unlike group A and group B chemokines, CCL7 and CXCL10 displayed weak binding with non-sulfated and phosphate HS ligands (ranked between 2–56%). Among six di-sulfated ligands, only **HT-3S-NH** (ranked 78% for CCL7 and 65% for CXCL10) and **HT-6S-NAc** (ranked 73% for CCL7) displayed strong binding as compared to the other analogs. Similarly, among four tetra-sulfated HS ligand, **HT-2,3S-NH** (ranked 35% for CCL7 and 27% for CXCL10) displayed weak binding, whereas **HT-2,6S-NH** (ranked 91% for CCL7 and 89% for CXCL10), **HT-2,6S-NAc** (ranked 86% for CCL7 and 64% for CXCL10) and **HT-3,6S-NH** (ranked 89% for CCL7 and 96% for CXCL10) ligands displayed strong binding (Fig. 2a). These results illustrate that group C chemokines have some selectivity to di-sulfated ligands. Larger HS-disulfated library could further allow to fine-tune their binding patterns characteristics.

Finally, all members of D group chemokines (CXCL8, CCL5 and CCL2) displayed exclusive strong binding to high-sulfated ligands and weak binding with di-sulfated ligands, nonsulfated or phosphorylated ligands. Among high-sulfate ligands, group D chemokines displayed high selectivity to NU domain over NA domain. Notably, CXCL8 and CCL2 displayed strong binding preference to **HT-3,6S-NH** (ranked 94% for CXCL8 and 95% for CCL2) ligand, whereas, CCL5 showed strong binding to **HT-2,6S-NH** (ranked 95%) ligand (Fig. 2a), suggesting that NU domain is highly significant in modulating these chemokines activities, particularly of group D chemokines. It had previously been shown that the interaction of heparin tetrasaccharides with CCL5 is modulated by sulfation pattern and pH, however these studies also emphasized the dynamic and often non-specific nature of the ionic GAG-protein contacts.[15] Nevertheless, to provide further insights into the interactions between CCL5 and HT compounds of varying sulfation patterns, we used a co-crystal structure of CCL5 co-complexed with a heparin trisaccharide (PDB ID: 5DNF, Chain I), in which sulfate groups were added or deleted from the ligand (Fig. 2b). This analysis revealed that sulfation at the 6 position in GlcNH is preferred over sulfation at the 3 position, because the 6S group can interact with both R59 and K55, whereas the 3S only interacts with R59. For this reason, both GlcNH[6S]-IdoA[2S]-GlcNH[6S] and GlcNH[3S,6S]-IdoA-GlcNH[3S,6S] (related to **HT-2,6S-NH** and **HT-3,6S-NH**, ranked 95% and 82% by glycan microarrays, respectively) are stronger

(a)

Substituent	Structure	Group ID	A CCL13	A CCL21	A CXCL12	B CCL28	C CCL7	C CXCL10	D CXCL8	D CCL5	D CCL2
None	GlcNAcα(1-4)IdoAα(1-4)GlcNAcα(1-4)IdoA-proNH2	HT-0S-NAc	24	27	16	22	2	14	3	1	0
	GlcNHα(1-4)IdoAα(1-4)GlcNHα(1-4)IdoA-proNH2	HT-0S-NH	64	62	51	36	45	39	13	3	3
IdoA(2S)	GlcNAcα(1-4)IdoA(2S)α(1-4)GlcNAcα(1-4)IdoA(2S)-proNH2	HT-2S-NAc	21	23	11	21	1	11	2	1	0
	GlcNHα(1-4)IdoA(2S)α(1-4)GlcNHα(1-4)IdoA(2S)-proNH2	HT-2S-NH	70	69	69	43	56	52	37	31	13
GlcNAc(6S)	GlcNAc(6S)α(1-4)IdoAα(1-4)GlcNAc(6S)α(1-4)IdoA-proNH2	HT-6S-NAc	81	79	66	79	73	41	19	24	13
GlcNH(6S)	GlcNH(6S)α(1-4)IdoAα(1-4)GlcNH(6S)α(1-4)IdoA-proNH2	HT-6S-NH	45	25	25	38	11	15	5	3	1
GlcNAc(6P)	GlcNAc(6P)α(1-4)IdoAα(1-4)GlcNAc(6P)α(1-4)IdoA-proNH2	HT-6P	70	81	75	39	40	48	10	5	1
GlcNAc(6S)-IdoA(2S)	GlcNAc(6S)α(1-4)IdoA(2S)α(1-4)GlcNAc(6S)α(1-4)IdoA(2S)-proNH2	HT-2,6S-NAc	79	71	69	66	86	64	53	54	30
GlcNH(6S)-IdoA(2S)	GlcNH(6S)α(1-4)IdoA(2S)α(1-4)GlcNH(6S)α(1-4)IdoA(2S)-proNH2	HT-2,6S-NH	74	66	79	79	91	89	79	95	80
GlcNAc(6P)-IdoA(2P)	GlcNAc(6P)α(1-4)IdoA(2P)α(1-4)GlcNAc(6P)α(1-4)IdoA(2P)-proNH2	HT-6,2P	87	78	59	78	56	55	29	14	2
GlcNH(3S)	GlcNH(3S)α(1-4)IdoAα(1-4)GlcNH(3S)α(1-4)IdoA-proNH2	HT-3S-NH	58	83	84	62	78	65	51	20	28
GlcNH(3S, 6S)	GlcNH(3S,6S)α(1-4)IdoAα(1-4)GlcNH(3S,6S)α(1-4)IdoA-proNH2	HT-3,6S-NH	69	73	80	54	89	96	94	82	95
GlcNH(3S)-IdoA(2S)	GlcNH(3S)α(1-4)IdoA(2S)α(1-4)GlcNH(3S)α(1-4)IdoA(2S)-proNH2	HT-2,3S-NH	64	48	45	66	35	27	9	4	1

%
100
75
50
25
0

(b)

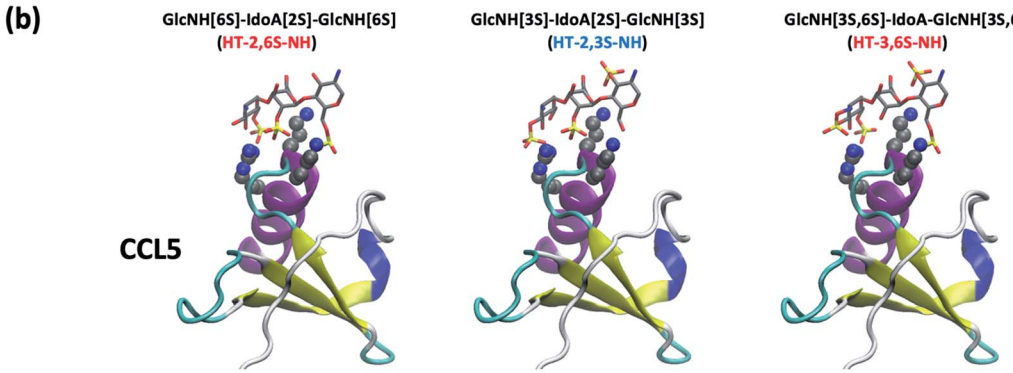

Fig. 2 Chemokine glycan microarray binding assay. (a) Arrays were fabricated on epoxide-activated slides as described.[16] Binding was tested at 3 serial dilutions, then detected with the relevant biotinylated secondary antibody (1 μg ml^{-1}) followed by Cy3-streptavidin (1.5 μg ml^{-1}) (Table S1†). Arrays were scanned, relative fluorescent units (RFU) obtained, and maximum RFU determined and set as 100% binding. Then rank binding (per printed glycan per concentration, per each chemokine dilution, per printed block) was determined. Since each glycans was printed at 2 concentration, 100% binding was set separately for each concentration. Then, binding to all the other glycans at the same concentration was ranked in comparison to the maximal binding, and the average rank binding and SEM for each glycan across the two glycan concentrations and three examined dilutions of each chemokine was calculated ($n = 6$; 2 glycan concentrations, across 3 chemokine dilutions). This analysis allowed to compare the glycan binding profiles of the different chemokines and dissect their binding preferences. The mean rank is shown as a heat map of all the examined binding assays together (red highest, blue lowest and white 50th percentile of ranking). (b) Sulfate groups were added or deleted from the ligand in the crystal structure of the co-complex of a heparin trisaccharide with CCL5 (PDB ID: 5DNF, Chain I) using Chimera (UCSF Chimera – a visualization system for exploratory research and analysis).[17] No other changes to the orientation of the ligand or protein were made. Based on glycan microarray screening, binding to CCL5 was high for GAG fragments HT-2,6-NH and HT-3,6S-NH (red), but low to HT-2,3S-NH (blue), consistent with expectations based on the co-complex crystal structure models.

binders than GlcNH[3S]-IdoA[2S]-GlcNH[3S] (related to **HT-2,3S-NH**, ranked 4%) (Fig. 2a).

To quantitatively evaluate the binding patterns between HS ligands and chemokines, SPR experiment was performed with **H-3,6S-NH** and chemokines (CXCL10, CXCL8, CCL5 and CCL2), which showed strong selective and sensitive binding in microarray experiments. The equilibrium binding constants (K_D) measured from steady state fits are listed in Table S2.† **HT-3,6S-NH** displayed strong binding with inflammatory chemokine CCL2 (1.89 μM) (Fig. 3a–d). This strong binding is attributed to the fast association (K_{on}) as compared to chemokine–CCL2 interaction. In contrast, **HT-2,6SNH** displayed strong binding to CCL5 (2.34 μM) (Fig. 3a–d). Interestingly, CXCL8, CCL7 and CXCL10 showed weak binding constants (10–15 μM) for both NU domain ligands (Fig. S2†). Furthermore, SPR analysis of CCL5 and CCL2 displayed 3-fold stronger binding with **H-3,6S-NH** and **HT-2,6S-NH** ligands, respectively. Thus, for the first time, we were able to identify key NU domain sulfation pattern that can modulate chemokines activity.

Given the high affinity binding of **HT-3,6S-NH** to CCL2 chemokines, and the link between CCL2 and cancer metastasis, investigating inhibitor effect on CCL2 cancer cell signaling is considered a novel approach to demonstrate the therapeutic potential of HS mimetics.[18] To this end, we first studied cancer cells proliferation in the presence of **HT-3,6S-NH** (**H-3**) ligand and CCL2. Native heparin was used as a positive control. Cell proliferation was analyzed by WST assay using MCF-7 cell line, as they express high level of the CCL2 specific chemokine receptor (CCR2).[19] It was observed that high concentration of **HT-3,6S-NH** ligand moderately inhibited cell proliferation (Fig. 3e). To understand the mechanism of inhibition, we performed cell-cycle analysis in the presence and absence of HS ligand and

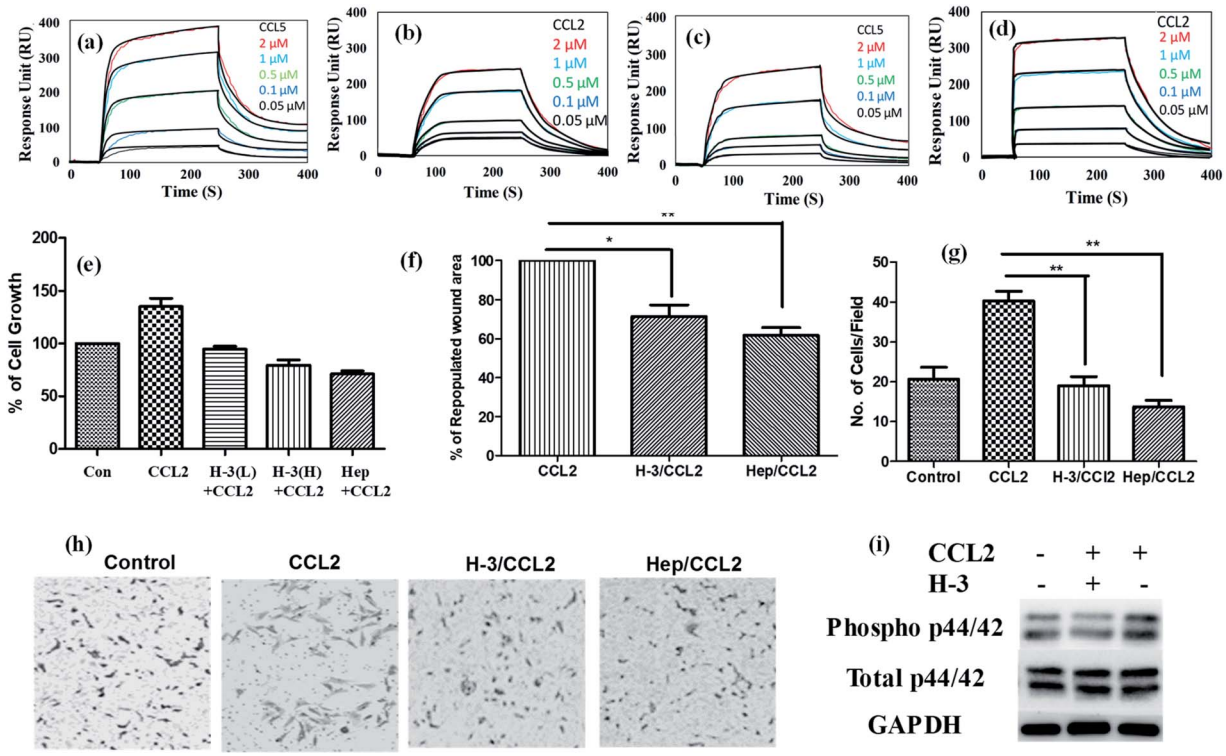

Fig. 3 SPR analysis of chemokines binding profile on sensor chip having HT ligands: (a & b) SPR binding analysis of the interaction between **HT-2,6S-NH** with CCL5 and CCL2 respectively; (c & d) SPR binding analysis of the interaction between **HT-3,6S-NH** with CCL5 and CCL2, respectively. Concentrations of chemokines were 0.05–2 μM. A global fit according to a 1 : 1 binding model was applied (black curves); (e) MCF-7 cell proliferation was quantified by WST assay after 72 h treatment with **HT-3,6S-NH** (**H-3**) at different concentration with CCL2 chemokine. The bar graphs indicated percentage of cell growth. L corresponds to 10 μg ml^{-1} concentration; H corresponds to 50 μg ml^{-1} concentration of ligands ((**H-3**) and Heparin (**Hep**)). **CCL2** chemokines (50 ng); (f) cell migration assay: area repopulated in 8 h with CCL2 chemokine is considered as 100% wound heal and data expressed as mean ± SD ($n = 3$; $^*P < 0.05$, $^*P < 0.01$); (g) Boyden chamber assay was performed in presence of **HT-3,6S-NH** and **Hep** (50 μg ml^{-1}) with or without CCL2 (50 ng); (h) bright field images of Boyden chamber assay; (i) MAPK pathway analysis: MCF-7 cells were treated with **CCL2** (50 ng) with or without **HT-3,6S-NH** (**H-3**) ligands (50 μg ml^{-1}) and cell lysate was prepared at 30 min time points and P-p44/42 and total p44/42 was imaged.

CCL2 chemokine, then quantified the DNA content of each cell state by flow-cytometry. The cell cycle analysis clearly revealed that addition of CCL2 induced S and G2/M phase cell-cycles, while high concentration of **HT-3,6S-NH** and heparin reduced G2/M state from 15% to 10%, indicating that **HT-3,6S-NH** moderately to poorly activate the cell cycle. Further studies with **HT-3,6S-NH** multivalent probes are ideal for modulating cancer cell proliferation.

We next examined cell migration by wound healing assay (Fig. 3f) and by Boyden-chamber assay (Fig. 3g and h). Addition of **HT-3,6S-NH** ligand reduced chemokine activity, where a 24% reduction in cell migration rate and 41% reduction in the wound healing was observed. In addition, a substantial reduction in cell migration was observed in the Boyden chamber assay. Finally, the mechanism of invasiveness was examined further by analyzing the level of phosphorylation of MAP kinase pathway. Western blot analysis of p42/44 showed that MCF-7 cells treated with **HT-3,6S-NH**/CCL2 expressed low level of MAPK compared to CCL2 treated cells (Fig. 3i). Overall, these results suggest that **HT-3,6S-NH** is a potential ligand that can modulate CCL2 chemokine activities.

Conclusions

Here, we describe the divergent synthesis of 13 new HS ligands, displaying different sulfate/phosphate patterns with NU/NA glucosamine residues. The binding interactions between HS ligands and chemokines on nano-printed microarray platform displayed several cryptic binding pockets for sulfation patterns with NU domain, which was not identified with previous HS synthetic ligands. Among them, **HT-3,6S-NH** ligand displayed a marked selectivity and sensitivity to CCL2 chemokine. The biological relevance of such structural binding studies was illustrated by incubating **HT-3,6S-NH** ligand with cancer cells showing the HS ligand inhibited cancer cells proliferation, migration and invasion. Thus, NU domain is important to regulate specific chemokine biological activities, thereby demonstrating potential novel therapeutic applications of HS ligands. To the best of our knowledge, we have identified CCL2 and CCL5 chemokines as only the fourth and fifth proteins currently known to recognize NU-domain HS ligands with different sulfation patterns.

Conflicts of interest

There are no conflicts of interest to declare.

Acknowledgements

Financial support from the IISER, Pune, DST (Grant No. SR/NM/NS-1113/2016), DBT (Grant No. BT/PR21934/NNT/28/1242/2017, STARS/APR2019/CS/426/FS, and SERB/F/9228/2019-2020) are gratefully acknowledged (to R. K.). This work was supported by the Israeli Science Foundation (ISF; to V. P.-K.). We would also like to thank Prof. John Gallagher for his contribution to heparin chemistry. This work is dedicated to Prof. J. D. Esko for his contribution to heparan sulfate glycobiology.

Notes and references

1 (*a*) A. Mantovani, R. Bonecchi and M. Locati, *Nat. Rev. Immunol.*, 2006, **6**, 907–918; (*b*) C. R. Mackay, *Nat. Immunol.*, 2001, **2**, 95–101; (*c*) R. J. Nibbs and G. J. Graham, *Nat. Rev. Immunol.*, 2013, **13**, 815–829; (*d*) B. Moser and P. Loetscher, *Nat. Immunol.*, 2001, **2**, 123–128; (*e*) A. Mortier, J. Van Damme and P. Proost, *Immunol. Lett.*, 2012, **145**, 2–9.

2 (*a*) K. Jöhrer, L. Pleyer, A. Olivier, E. Maizner, C. Zelle-Rieser and R. Greil, *Expert Opin. Biol. Ther.*, 2008, **8**, 269–290; (*b*) W. G. Liang, C. G. Triandafillou, T.-Y. Huang, M. M. L. Zulueta, S. Banerjee, A. R. Dinner, S.-C. Hung and W.-J. Tang, *Proc. Natl. Acad. Sci. U. S. A.*, 2016, **113**, 5000–5005; (*c*) D. P. Dyer, C. L. Salanga, B. F. Volkman, T. Kawamura and T. M. Handel, *Glycobiology*, 2016, **26**, 312–326; (*d*) L. Wang, M. Fuster, P. Sriramarao and J. D. Esko, *Nat. Immunol.*, 2005, **6**, 902–910; (*e*) C. R. Parish, *Nat. Rev. Immunol.*, 2006, **6**, 633–643.

3 (*a*) A. E. Proudfoot, T. M. Handel, Z. Johnson, E. K. Lau, P. LiWang, I. Clark-Lewis, F. Borlat, T. N. Wells and M. H. Kosco-Vilbois, *Proc. Natl. Acad. Sci. U. S. A.*, 2003, **100**, 1885–1890; (*b*) Z. Johnson, A. Proudfoot and T. Handel, *Cytokine Growth Factor Rev.*, 2005, **16**, 625–636.

4 K. M. Sepuru and K. Rajarathnam, *J. Biol. Chem.*, 2019, **294**, 15650–15661.

5 S. E. Stringer and J. T. Gallagher, *J. Biol. Chem.*, 1997, **272**, 20508–20514.

6 D. Spillmann, D. Witt and U. Lindahl, *J. Biol. Chem.*, 1998, **273**, 15487–15493.

7 G. C. Jayson, S. U. Hansen, G. J. Miller, C. L. Cole, G. Rushton, E. Avizienyte and J. M. Gardiner, *Chem. Commun.*, 2015, **51**, 13846–13849.

8 G. J. Sheng, Y. I. Oh, S.-K. Chang and L. C. Hsieh-Wilson, *J. Am. Chem. Soc.*, 2013, **135**, 10898–10901.

9 J. L. de Paz, E. A. Moseman, C. Noti, L. Polito, U. H. von Andrian and P. H. Seeberger, *ACS Chem. Biol.*, 2007, **2**, 735–744.

10 C. Zong, A. Venot, X. Li, W. Lu, W. Xiao, J.-S. L. Wilkes, C. L. Salanga, T. M. Handel, L. Wang, M. A. Wolfert and G. J. Boons, *J. Am. Chem. Soc.*, 2017, **139**, 9534–9543.

11 (*a*) T. Toida, H. Yoshida, H. Toyoda, I. Koshiishi, T. Imanari, R. E. Hileman, J. R. Fromm and R. J. Linhardt, *Biochem. J.*, 1997, **322**, 499–506; (*b*) C. Westling and U. Lindahl, *J. Biol. Chem.*, 2002, **277**, 49247–49255.

12 (*a*) C. Vanpouille, A. Deligny, M. Delehedde, A. Denys, A. Melchior, X. Liénard, M. Lyon, J. Mazurier, D. G. Fernig and F. Allain, *J. Biol. Chem.*, 2007, **282**, 24416–24429; (*b*) Z. Wei, M. Lyon and J. T. Gallagher, *J. Biol. Chem.*, 2005, **280**, 15742–15748; (*c*) Z. Wei, J. A. Deakin, B. S. Blaum, D. Uhrín, J. T. Gallagher and M. Lyon, *Glycoconjugate J.*, 2011, **28**, 525–535; (*d*) A. Koenig, K. Norgard-Sumnicht, R. Linhardt and A. Varki, *J. Clin. Invest.*, 1998, **101**, 877–889; (*e*) K. Norgard-Sumnicht and A. Varki, *J. Biol. Chem.*, 1995, **270**, 12012–12024.

13 (*a*) M. Mende, C. Bednarek, M. Wawryszyn, P. Sauter, M. B. Biskup, U. Schepers and S. Bräse, *Chem. Rev.*, 2016, **116**, 8193–8255; (*b*) W. Lu, C. Zong, P. Chopra, L. E. Pepi, Y. Xu, I. J. Amster, J. Liu and G. J. Boons, *Angew. Chem., Int. Ed.*, 2018, **57**, 5340–5344; (*c*) S. U. Hansen, G. J. Miller, M. J. Cliff, G. C. Jayson and J. M. Gardiner, *Chem. Sci.*, 2015, **6**, 6158–6164; (*d*) Y. P. Hu, S. Y. Lin, C. Y. Huang, M. M. L. Zulueta, J. Y. Liu, W. Chang and S. C. Hung, *Nat. Chem.*, 2011, **3**, 557–563; (*e*) X. Zhang, V. Pagadala, H. M. Jester, A. M. Lim, T. Q. Pham, A. M. P. Goulas, J. Liu and R. J. Linhardt, *Chem. Sci.*, 2017, **8**, 7932–7940; (*f*) C. Noti, J. L. de Paz, L. Polito and P. H. Seeberger, *Chem. - Eur. J.*, 2006, **12**, 8664–8686; (*g*) J. L. de Paz, C. Noti and P. H. Seeberger, *J. Am. Chem. Soc.*, 2006, **128**, 2766–2767; (*h*) Y.-P. Hu, Y.-Q. Zhong, Z.-G. Chen, C.-Y. Chen, Z. Shi, M. M. L. Zulueta, C.-C. Ku, P.-Y. Lee, C.-C. Wang and S.-C. Hung, *J. Am. Chem. Soc.*, 2012, **134**, 20722–20727; (*i*) N. J. Pawar, L. Wang, T. Higo, C. Bhattacharya, P. K. Kancharla, F. Zhang, K. Baryal, C. X. Huo, J. L. Jian, R. J. Linhardt, X. H. Xuefei and L. C. Hsieh-Wilson, *Angew. Chem., Int. Ed.*, 2019, **58**, 18577–18583; (*j*) R. S. Boothello, A. Sarkar, V. M. Tran, T. K. Nguyen, N. V. Sankaranarayanan, A. Y. Mehta, A. Alabbas, S. Brown, A. Rossi, A. C. Joice, C. P. Mencio, M. V. Quintero, B. Kuberan and U. R. Desai, *ACS Chem. Biol.*, 2015, **10**, 1485–1494; (*k*) N. V. Sankarayanarayanan, T. R. Strebel, R. S. Boothello, K. Sheerin, A. Raghuraman, F. Sallas, P. D. Mosier, N. D. Watermeyer, S. Oscarson and U. R. Desai, *Angew. Chem., Int. Ed.*, 2017, **56**, 2312–2317; (*l*) L. Sun, P. Chopra and G.-J. Boons, *J. Org. Chem.*, 2020, **85**(24), 16082–16098; (*m*) S. Arungundram, K. Al-Mafraji, J. Asong, F. E. Leach III, I. J. Amster, A. Venot, J. E. Turnbull and G.-J. Boons, *J. Am. Chem. Soc.*, 2009, **131**, 17394–17405; (*n*) N. V. Sankaranarayanan, T. R. Strebel, R. S. Boothello, K. Sheerin, A. Raghuraman, F. Sallas, P. D. Mosier, N. D. Watermeyer, S. Oscarson and U. R. Desai, *Angew. Chem., Int. Ed.*, 2017, **56**, 2312–2317; (*o*) C. H. Chang, L. S. Lico, T. Y. Huang, S. Y. Lin, C. L. Chang, S. D. Arco and S. C. Hung, *Angew. Chem., Int. Ed.*, 2014, **126**, 10034–10037; (*p*) T. N. Laremore, F. Zhang, J. S. Dordick, J. Liu and R. J. Linhardt, *Curr. Opin. Chem. Biol.*, 2009, **13**, 633–640; (*q*) S. B. Dulaney and X. Huang, *Adv. Carbohydr. Chem. Biochem.*, 2012, **67**, 95–136; (*r*)

S. U. Hansen, G. J. Miller, G. C. Jayson and J. M. Gardiner, *Org. Lett.*, 2013, **15**, 88–91.

14 (*a*) C. D. Shanthamurthy and R. Kikkeri, *Eur. J. Org. Chem.*, 2019, **2019**, 2950–2953; (*b*) S. Anand, S. Mardhekar, R. Raigawali, N. Mohanta, P. Jain, C. D. Shanthamurthy, B. Gnanaprakasam and R. Kikkeri, *Org. Lett.*, 2020, **22**, 3402–3406.

15 A. Singh, W. C. Kett, I. C. Severin, I. Agyekum, J. Duan, I. J. Amster, A. E. Proudfoot, D. R. Coombe and R. J. Woods, *J. Biol. Chem.*, 2015, **290**, 15421–15436.

16 (*a*) V. Padler-Karavani, X. Song, H. Yu, N. Hurtado-Ziola, S. Huang, S. Muthana, H. A. Chokhawala, J. Cheng, A. Verhagen and M. A. Langereis, *J. Biol. Chem.*, 2012, **287**, 22593–22608; (*b*) S. L. Ben-Arye, H. Yu, X. Chen and V. Padler-Karavani, *J. Visualized Exp.*, 2017, e56094; (*c*) M. Gade, C. Alex, S. L. Ben-Arye, J. T. Monteiro, S. Yehuda, B. Lepenies, V. Padler-Karavani and R. Kikkeri, *Chembiochem*, 2018, **19**, 1170–1177; (*d*) C. D. Shanthamurthy, P. Jain, S. Yehuda, J. T. Monteiro, S. L. Ben-Arye, B. Subramani, B. Lepenies, V. Padler-Karavani and R. Kikkeri, *Sci. Rep.*, 2018, **8**, 1–7.

17 E. F. Pettersen, T. D. Goddard, C. C. Huang, G. S. Couch, D. M. Greenblatt, E. C. Meng and T. E. Ferrin, *J. Comput. Chem.*, 2004, **25**, 1605–1612.

18 Y. Lu, Z. Cai, G. Xiao, Y. Liu, E. T. Keller, Z. Yao and J. Zhang, *J. Cell. Biochem.*, 2007, **101**, 676–685.

19 P. Dutta, M. Sarkissyan, K. Paico, Y. Wu and J. V. Vadgama, *Breast Cancer Res. Treat.*, 2018, **170**, 477–486.